



Synthesis and reactivity of 2-(*tert*-butylcyclopentadienyl)-indenyl dinuclear ruthenium complex $[\eta^5:\eta^5-(^t\text{BuC}_5\text{H}_3)(\text{C}_9\text{H}_6)]\text{Ru}_2(\text{CO})_4$: Halogen induced Ru cleavage from indenyl ring

Bin Li, Xing Tan, Shansheng Xu, Haibin Song, Baiquan Wang*

State Key Laboratory of Elemento-Organic Chemistry, College of Chemistry, Nankai University, Weijin Road 94#, Tianjin 300071, People's Republic of China

ARTICLE INFO

Article history:

Received 6 October 2008
Received in revised form 24 December 2008
Accepted 26 December 2008
Available online 3 January 2009

Keywords:

Unsymmetrical fulvalene
Indene
Ruthenium
Cleavage reactions
Halogen

ABSTRACT

Thermal reaction of $\text{Ru}_3(\text{CO})_{12}$ with unsymmetrical Fv ligand 2-(*tert*-butylcyclopentadienyl)-indene provided $[\eta^5:\eta^5-(^t\text{BuC}_5\text{H}_3)(\text{C}_9\text{H}_6)]\text{Ru}_2(\text{CO})_4$ (**2**) in good yield. When **2** reacted with three or more equivalent of halogen X_2 , compounds $[(\eta^5-^t\text{BuC}_5\text{H}_3)(\text{C}_9\text{H}_6\text{X})]\text{Ru}(\text{CO})_2\text{X}$ ($\text{X} = \text{Br}$, **3**; I , **4**) were isolated in moderate yield. In complexes **3** and **4** only the Cp rings were coordinated with $\text{Ru}(\text{CO})_2\text{X}$, along with uncomplexed halogenated-indenyl rings. All the new complexes have been fully characterized. X-ray characterization of **2**, **3**, and **4** are also provided.

© 2009 Elsevier B.V. All rights reserved.

1. Introduction

Dinuclear fulvalene $[\eta^5:\eta^5\text{-CpCp (Fv, Cp = C}_5\text{H}_4\text{, cyclopentadienyl ring)]$ complexes, in which the Cp moieties are directly attached to each other without a bridging group, have been extensively explored in the last two decades [1–4]. Fulvalene can act as good ligand for many bimetallic complexes in part due to the strong bonding of its Cp rings to transition metals. The properties of Fv bimetallic complexes are quite different from those of Cp analogues might attribute to several reasons: (a) the Fv ligands act as frameworks for dinuclear metal complexes that are resistant to fragmentation and maintain two metal centers in close proximity even after the M–M bond cleavage; (b) the Fv ligands are forced to bend away from planarity to accommodate the M–M bonds, and the resulting distortions of the ligands in turn cause unique reactivity; (c) the two metal centers can communicate through the π -bond system of the Fv ligand regardless whether the existence of M–M bond or not, and whether the metals are oriented *cis* or *trans* with respect to the ligand [1,3,5].

The process for the haptotropic rearrangement of coordinated cyclic polyenyl ligand is casually termed “ring slippage” and has been reviewed for the cyclopentadienyl (Cp) and indenyl (Ind) ligands [6,7]. Transition metal complexes containing the indenyl ligand have received much attention due to their enhanced reactivity and catalytic ability as compared to the cyclopentadienyl

analogues. Basolo and co-workers called this phenomenon the “indenyl effect” [8]. They attributed it to the ease of slippage from a nominally 18-electron η^5 structure to a 16-electron η^3 species, assisted by restoration of full aromaticity to the benzene ring.

The indenyl analogue to Fv ligand – dibenzofulvalene – was reported with its iron and group 6 metal complexes by Kerber and Waldbaum [9,10]. Later, Gaede and Tews demonstrated the synthesis of bridged dibenzofulvalene ligand and its Mo, Fe, Co, Rh, and Ir complexes [11,12]. However, the fulvalene ligands with unsymmetrical backbones, such as 2-(cyclopentadienyl)-indenyl species, were less explored. Only two complexes *rac*-Fc($\eta^5\text{-C}_9\text{H}_6$)₂Fe and *rac*-Fc($\eta^5\text{-C}_9\text{H}_6$)₂ZrCl₂ based on such unsymmetrical Fv foundation were reported before [13].

In this study, we will report the synthesis of $[\eta^5:\eta^5-(^t\text{BuC}_5\text{H}_3)(\text{C}_9\text{H}_6)]\text{Ru}_2(\text{CO})_4$ (**2**) by reaction of 2-(*tert*-butylcyclopentadienyl)-indene (**1**) with $\text{Ru}_3(\text{CO})_{12}$ and its subsequent reactions with halogens (Br_2 , I_2). The latter reactions provide rare examples of halogen induced metal cleavage from indenyl ring.

2. Experimental

2.1. General considerations

Schlenk and vacuum line techniques were employed for all manipulations. All solvents were distilled from appropriate drying agents under argon prior to use. Melting points were uncorrected. ¹H NMR spectra were recorded on a Bruker AV300, or Varian Mercury VX300, or Varian Mercury Plus 400 instrument. IR spectra

* Corresponding author. Tel./fax: +86 22 23504781.
E-mail address: bqwang@nankai.edu.cn (B. Wang).

were recorded as KBr disks on a Nicolet 380 FT-IR spectrometer. Elemental analyses were performed on a Perkin-Elmer 240C analyzer. 2-(*tert*-Butylcyclopentadienyl)-indene (**1**) [14] were prepared according to the literature method.

2.2. Reaction of **1** with $\text{Ru}_3(\text{CO})_{12}$ and synthesis of $[\eta^5\text{-}\eta^5\text{-}(\text{}^t\text{BuC}_5\text{H}_3)(\text{C}_9\text{H}_6)]\text{Ru}_2(\text{CO})_4$ (**2**)

A solution of **1** (94 mg, 0.40 mmol) and $\text{Ru}_3(\text{CO})_{12}$ (160 mg, 0.25 mmol) in toluene (30 mL) was refluxed for 6 h. After removal of solvent the residue was chromatographed on an alumina column. Elution with petroleum ether– CH_2Cl_2 (3/1, v/v) gave a yellow band, which afforded **2** (128 mg, 62% yield) as yellow crystals. M.p. 243 °C (dec.). Anal. Calc. for $\text{C}_{22}\text{H}_{18}\text{O}_4\text{Ru}_2$: C, 48.17; H, 3.11. Found: C, 48.36; H, 3.48%. ^1H NMR (CDCl_3 , 300 MHz) δ 7.34 (m, 2H, Ar-H), 7.19 (m, 2H, Ar-H), 5.53 (m, 1H, Cp-H), 4.63 (s, 2H, Ind-CH), 4.15 (t, 1H, Cp-H), 4.04 (s, 1H, Cp-H), 1.22 (m, 9H, CMe_3); IR (ν_{CO} , cm^{-1}): 2006(s), 1952(s).

2.3. Reaction of complex **2** with Br_2 and synthesis of $[(\eta^5\text{-}^t\text{BuC}_5\text{H}_3)(\text{C}_9\text{H}_6\text{Br})]\text{Ru}(\text{CO})_2\text{Br}$ (**3**)

A solution of complex **2** (60 mg, 0.110 mmol) and Br_2 (0.33 mmol, ~5% solution in benzene) in benzene (30 mL) was stirred for 2 h at room temperature. The reaction was monitored by TLC and stopped when complex **2** was used up completely. After removal of solvent the residue was chromatographed on a silica column using CH_2Cl_2 as eluent, which afforded complex **3** (25 mg, 41% yield) as yellow crystals as a mixture of two isomers in ~3:2 ratio at 20 °C. M.p. 157–158 °C. Anal. Calc. for $\text{C}_{20}\text{H}_{18}\text{Br}_2\text{O}_2\text{Ru}$: C, 43.58; H, 3.29. Found: C, 43.31; H, 3.45%. ^1H NMR (CDCl_3 , 400 MHz): For isomer **a**, δ 7.52 (m, 1H, Ar-H), 7.33 (m, 1H, Ar-H), 7.30 (m, 2H, Ar-H), 7.13 (m, 1H, $\text{CH}=\text{CCHBr}$), 5.88 (br s, 1H, $\text{CH}=\text{CCHBr}$), 5.74 (br s, 1H, Cp-H), 5.64 (br s, 1H, Cp-H), 5.35 (br s, 1H, Cp-H), 1.26 (m, 9H, CMe_3). For isomer **b**, δ 7.52 (m, 1H, Ar-H), 7.33 (m, 1H, Ar-H), 7.30 (m, 2H, Ar-H), 7.12 (m, 1H, $\text{CH}=\text{CCHBr}$), 5.98 (br s, 1H, $\text{CH}=\text{CCHBr}$), 5.60 (br s, 1H, Cp-H), 5.52 (br s, 1H, Cp-H), 5.30 (br s, 1H, Cp-H), 1.27 (m, 9H, CMe_3); IR (ν_{CO} , cm^{-1}) of a mixture of isomers: 2035(s), 1986 (s).

2.4. Reaction of complex **2** with I_2 and synthesis of $[(\eta^5\text{-}^t\text{BuC}_5\text{H}_3)(\text{C}_9\text{H}_6\text{I})]\text{Ru}(\text{CO})_2\text{I}$ (**4**)

A solution of complex **2** (57 mg, 0.105 mmol) and I_2 (79 mg, 0.315 mmol) in benzene (30 mL) was stirred for 1 h at room temperature. The reaction was monitored by TLC and stopped when complex **2** was used up completely. After removal of solvent the residue was chromatographed on a silica column using petroleum ether– CH_2Cl_2 (1/1, v/v) as eluent, which afforded complex **4** (46 mg, 68% yield) as brown-red crystals as a mixture of two isomers in ~1:3 ratio at 20 °C. M.p. 140 °C (dec.). Anal. Calc. for $\text{C}_{20}\text{H}_{18}\text{I}_2\text{O}_2\text{Ru}$: C, 37.23; H, 2.81. Found: C, 37.00; H, 3.03%. ^1H NMR ($\text{C}_6\text{D}_6\text{CD}_3$, 300 M): For isomer **a**, δ 7.25 (br s, 1H, Ar-H), 6.98 (m, 1H, Ar-H), 6.94 (m, 2H, Ar-H), 6.71 (s, 1H, $\text{CH}=\text{CCHI}$), 5.71 (t, 1H, Cp-H), 5.50 (br s, 1H, $\text{CH}=\text{CCHI}$), 4.95 (m, 1H, Cp-H), 4.57 (m, 1H, Cp-H), 1.00 (s, 9H, CMe_3). For isomer **b**, δ 7.24 (d, $J = 3.21$ Hz, 1H, Ar-H), 6.99 (m, 1H, Ar-H), 6.96 (br s, 2H, Ar-H), 6.57 (s, 1H, $\text{CH}=\text{CCHI}$), 5.74 (s, 1H, $\text{CH}=\text{CCHI}$), 5.43 (m, 1H, Cp-H), 5.32 (t, 1H, Cp-H), 4.62 (m, 1H, Cp-H), 0.93 (s, 9H, CMe_3). IR (ν_{CO} , cm^{-1}) of a mixture of isomers: 2039(s), 1987 (s).

2.5. Crystallographic studies

Single crystals of all complexes suitable for X-ray diffraction were obtained from hexane/ CH_2Cl_2 . Data collection of complexes **2** and **4** were performed on a Bruker SMART 1000 at 294(2) K,

Table 1
Summary of crystallographic data for **2** · 0.5 CH_2Cl_2 , **3**, and **4**.

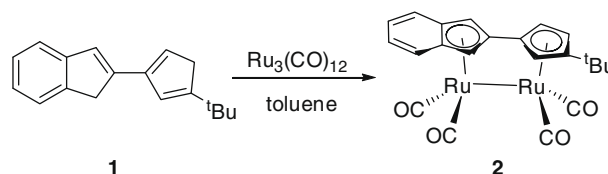
	2 · 0.5 CH_2Cl_2	3	4
Empirical formula	$\text{C}_{22.50}\text{H}_{19}\text{ClO}_4\text{Ru}_2$	$\text{C}_{20}\text{H}_{18}\text{Br}_2\text{O}_2\text{Ru}$	$\text{C}_{20}\text{H}_{18}\text{I}_2\text{O}_2\text{Ru}$
Formula weight	590.97	551.23	645.21
Crystal system	Orthorhombic	Triclinic	Triclinic
Space group	<i>Fdd2</i>	<i>P1</i>	<i>P1</i>
<i>a</i> (Å)	23.254(4)	8.4827(17)	8.6348(17)
<i>b</i> (Å)	44.351(9)	8.9187(18)	8.6911(17)
<i>c</i> (Å)	8.4715(13)	13.671(3)	14.642(3)
α (°)	90	82.53(3)	80.41(3)
β (°)	90	78.08(3)	83.06(3)
γ (°)	90	72.36(3)	68.82(3)
<i>V</i> (Å ³)	8737(3)	961.8(3)	1008.0(3)
<i>Z</i>	16	2	2
<i>D</i> _{calc.} (g cm^{-3})	1.797	1.903	2.126
μ (mm^{-1})	1.531	4.979	3.850
<i>F</i> (000)	4656	536	608
Crystal size (mm)	0.22 × 0.20 × 0.14	0.14 × 0.14 × 0.10	0.12 × 0.10 × 0.08
Maximum 2θ (°)	50.04	50.04	55.74
Number of reflections collected	11176	5585	7213
Number of independent reflections	3859 [0.0427]	3381 [0.0501]	4718 [0.0481]
$[R_{\text{int}}]$			
Number of parameters	271	226	229
Goodness-of-fit on F^2	0.963	1.047	0.977
R_1, wR_2 [$I > 2\sigma(I)$]	0.0269, 0.0573	0.0491, 0.0984	0.0434, 0.1047
R_1, wR_2 (all data)	0.0344, 0.0610	0.0670, 0.1043	0.0563, 0.1097
Largest peak in final difference map (e Å^{-3})	0.300	1.357	1.669

while **3** was performed on a Rigaku Saturn 70 equipped with a rotating anode system at 113(2) K, using graphite-monochromated Mo $\text{K}\alpha$ radiation (ω -2 θ scans, $\lambda = 0.71073$ Å). Semiempirical absorption corrections were applied for all complexes. The structures were solved by direct methods and refined by full-matrix least-squares. All calculations were using the SHELXTL-97 program system. The molecular structure of **2** contained one CH_2Cl_2 of solvation. The crystal data and summary of X-ray data collection are presented in Table 1.

3. Results and discussion

3.1. Synthesis and X-ray structure of $[\eta^5\text{-}\eta^5\text{-}(\text{}^t\text{BuC}_5\text{H}_3)(\text{C}_9\text{H}_6)]\text{Ru}_2(\text{CO})_4$

Reaction of $\text{Ru}_3(\text{CO})_{12}$ with the unsymmetrical Fv ligand 2-(*tert*-butylcyclopentadienyl)-indene (**1**) in refluxing toluene afforded the normal Fv dinuclear ruthenium complex $[\eta^5\text{-}\eta^5\text{-}(\text{}^t\text{BuC}_5\text{H}_3)(\text{C}_9\text{H}_6)]\text{Ru}_2(\text{CO})_4$ (**2**) in good yield (Scheme 1). The reaction can be also conducted in heptane and xylene, just with relatively lower yields. Complex **2** has been completely characterized, including by a single crystal X-ray diffraction study. The ^1H NMR studies showed three multiplets for three Cp protons at δ 5.53, 4.15, and 4.04 ppm [15–17], a singlet for two five-membered ring protons



Scheme 1.

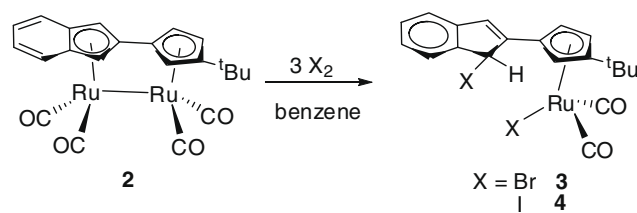
of indenyl at δ 4.63 ppm, an upfield singlet for the *tert*-butyl group, and two downfield multiplets for benzene ring. Only two terminal carbonyl absorptions were observed in its IR spectrum, suggesting the symmetry of the four CO groups.

As shown in Fig. 1, complex **2** contain a pair of ruthenium atoms linked by a metal–metal bond and an unsymmetrical Fv ligand, with four terminal carbonyls. There is no symmetry in the whole molecule, and complex **2** represents one of the two enantiomers. The structure of **2** is characterized by the large bend of the Fv ligand, defined as the angle between the Cp and indenyl rings (22.1°) and the long Ru–Ru bond distance [2.8277(6) Å]. The latter makes CO bridging disadvantageous. These parameters are comparable to those observed for FvRu₂(CO)₄ [16] and [η^5 : η^5 -2,2'-(PhCH₂C₅H₃)₂]Ru₂(CO)₄ [18]. It is worth noting that no torsion angle of Cp(centroid)–Ru(2)–Ru(1)–Cp(indenyl)(centroid) (0.0°) in **2** is detected, whereas the corresponding torsion angles in FvRu₂(CO)₄ and [η^5 : η^5 -2,2'-(PhCH₂C₅H₃)₂]Ru₂(CO)₄ are 4.3° [16] and 17.3° [18], respectively. In contrast to the staggered configuration of carbonyl ligands in [η^5 : η^5 -2,2'-(PhCH₂C₅H₃)₂]Ru₂(CO)₄ [18] and (η^5 : η^5 -C₅H₄CH₂C₅H₄)Ru₂(CO)₄ [19], the carbonyls in **2** are essentially eclipsed (see the right drawing of Fig. 1), which was also observed in FvRu₂(CO)₄ [16]. The eclipsed configuration of carbonyl ligands of **2** is further confirmed by its IR spectrum. The staggered form of carbonyls in [η^5 : η^5 -2,2'-(PhCH₂C₅H₃)₂]Ru₂(CO)₄ possibly attributed to the effects of the two benzyl substituents. Furthermore, the Cp(centroid)–Ru(2) distance of 1.896(4) Å is a little shorter than Cp(indenyl)(centroid)–Ru(1) distance of 1.940(4) Å.

It is useful to examine the degree of distortion from η^5 to η^3 coordination in the discussion of η^5 -indenyl metal fragment (Indenyl)Ru(CO)₂. As described by Taylor, Marder, and co-workers, the degree of distortion can be discussed in terms of the slip-fold distortion parameters: slip distortion (Δ), hinge angle (HA), and fold angle (FA) [20]. The slip-fold distortion parameters in complex **2** are: slip distortion (Δ) = 0.116(4) Å, hinge angle = 3.7° , and fold angle = 6.1° . These values fall within the range for small distortion from a η^5 coordination mode [20].

3.2. Reactions of [η^5 : η^5 -(*t*-BuC₅H₃)(C₉H₆)]Ru₂(CO)₄ (**2**) with halogen X₂ (X = Br, I) and X-ray structure of [η^5 -(*t*-BuC₅H₃)(C₉H₆X)]Ru(CO)₂X

It is well-known that the dimeric Cp₂M₂(CO)₄ (M = Fe, Ru, Os) complexes react with halogens (X₂) to give metal(II) halide carbonyl complexes Cp⁺M(CO)₂X [21]. And no reactions of fulvalene dinuclear complexes with halogens were reported before. So we undertaken a study on the reaction of **2** with X₂ (X = Br, I). Treatment of complex **2** with an equivalent of halogen X₂ (X = Br, I) only provided unidentified products. When **2** reacted with three or more equivalent of X₂, compounds [η^5 -(*t*-BuC₅H₃)(C₉H₆X)]Ru



Scheme 2.

(CO)₂X (X = Br, **3**; I, **4**) were isolated as brown crystals in moderate yield (Scheme 2). Complexes **3** and **4** were fully characterized, including by single crystal X-ray diffraction analysis.

The ORTEP plots of complexes **3** and **4** are shown in Figs. 2 and 3, respectively. The selected bond lengths and angles are listed in Table 2. Complexes **3** and **4** have similar structures. Both compounds contain unsymmetrical Fv ligands with only the Cp rings were coordinated to Ru(CO)₂X, along with uncomplexed 1-halogenated-indenyl rings. The halogen atom is in the same side with the Ru(CO)₂X toward the Fv ligand. The corresponding C(13)–X(2) bond lengths are 1.977(7) Å (for **3**) and 2.188(6) Å (for **4**), respectively. Consequently the bonds C(12)–C(13) and C(12)–C(20) are double and single bonds, respectively. Among the Ru–C bonds of the Cp ring, Ru(1)–C(4) and Ru(1)–C(5) bonds are much longer than the other three and Ru(1)–C(5) bond is the longest. The indenyl ring plane and Cp plane are close to coplanar with a twist angle of 5.6° (for **3**) and 8.7° (for **4**), respectively. In addition, the C(5)–C(12) bond lengths [1.455(10) Å (for **3**) and 1.441(8) Å (for **4**)] are shorter than a C–C single bond, which is comparable to that of complex **2** [C(13)–C(14), 1.453(6) Å].

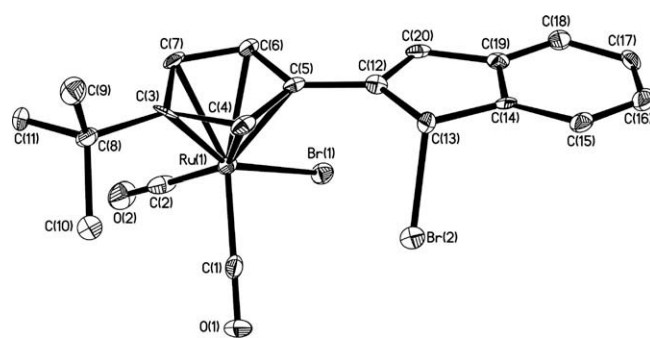


Fig. 2. ORTEP diagram of complex [η^5 -(*t*-BuC₅H₃)(C₉H₆Br)]Ru(CO)₂Br (**3**). Thermal ellipsoids are shown at the 30% level.

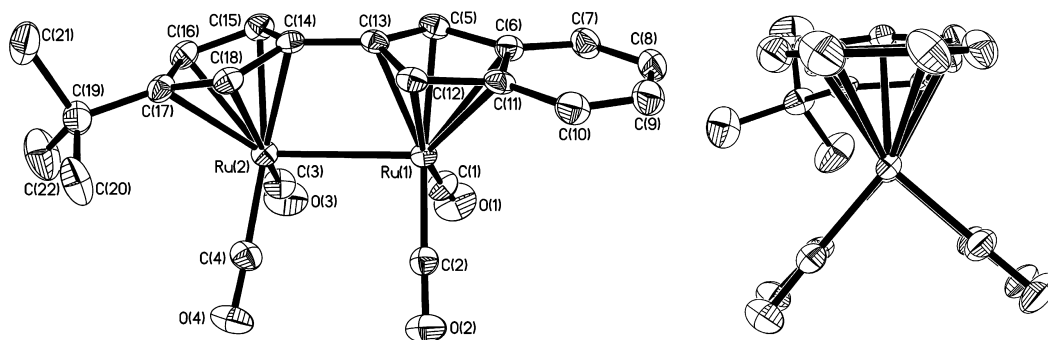


Fig. 1. ORTEP diagram of complex [η^5 : η^5 -(*t*-BuC₅H₃)(C₉H₆)]Ru₂(CO)₄ (**2**). Thermal ellipsoids are shown at the 30% level. The left drawing shows the view perpendicular to the Ru–Ru bond. The right drawing depicts the view down the Ru–Ru axis. Selected bond lengths [Å] and angles [°] are: Ru(1)–Ru(2) 2.8277(6), Ru(1)–C(5) 2.233(4), Ru(1)–C(6) 2.349(4), Ru(1)–C(11) 2.370(4), Ru(1)–C(12) 2.255(5), Ru(1)–C(13) 2.227(4), Ru(2)–Cp(centroid) 2.250, C(13)–C(14) 1.453(6), C(2)–Ru(1)–C(1) 88.9(2), C(4)–Ru(2)–C(3) 90.3(2), Ru(1)–Ru(2)–Cp(centroid) 105.57, Ru(2)–Ru(1)–Cp(indenyl)(centroid) 104.67.

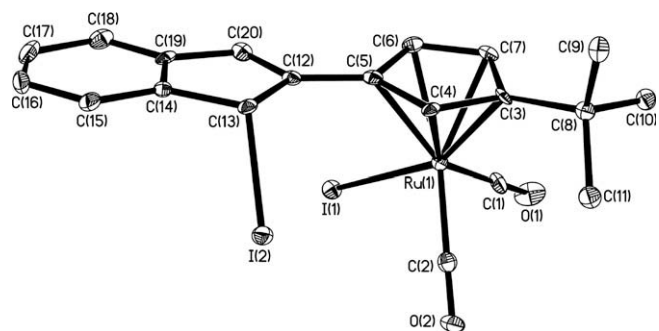
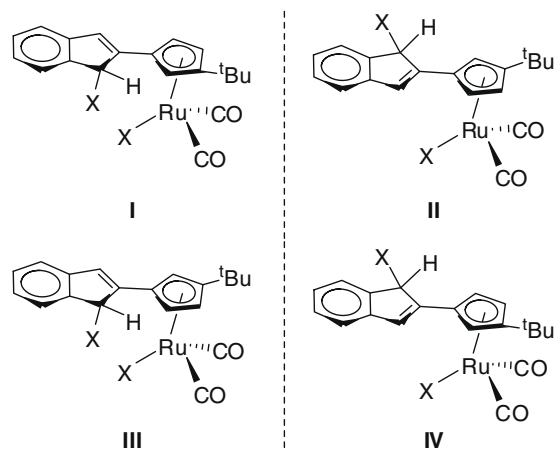


Fig. 3. ORTEP diagram of complex $[\eta^5\text{-}(\text{tBuC}_5\text{H}_3)(\text{C}_9\text{H}_6\text{I})\text{Ru}(\text{CO})_2\text{I}]$ (**4**). Thermal ellipsoids are shown at the 30% level.

Table 2

Selected bond lengths (Å) and angles (°) for **3** and **4**.

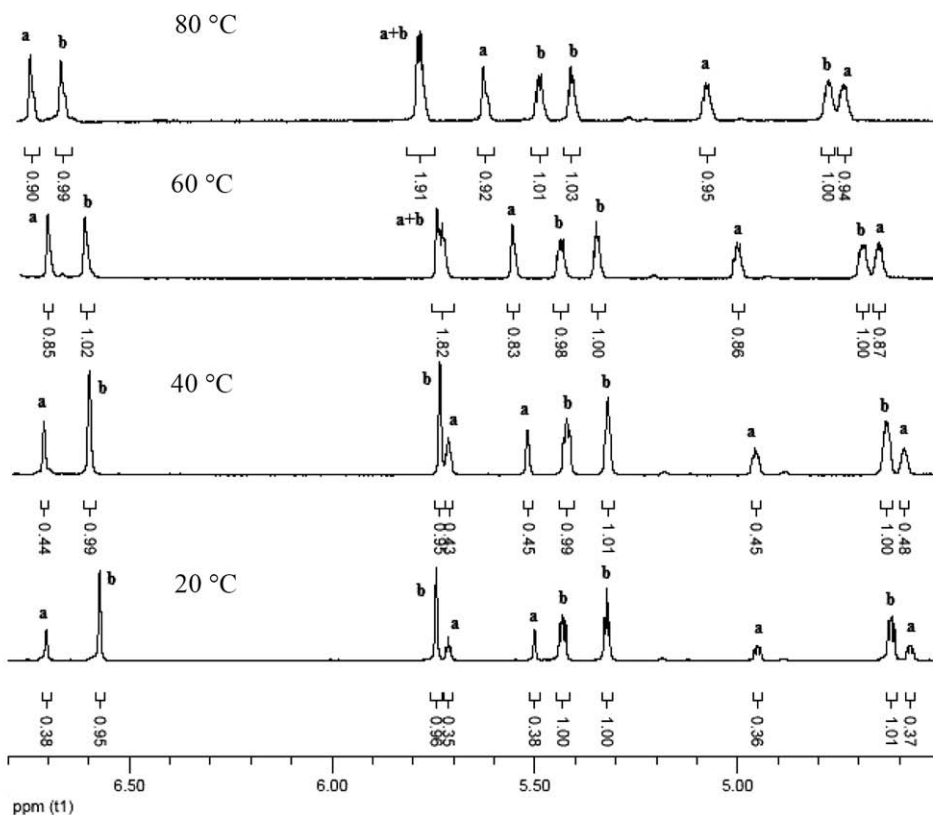
	3	4	3	4
Ru(1)–C(1)	1.898(8)	1.914(9)	Ru(1)–C(2)	1.872(8)
Ru(1)–C(3)	2.216(7)	2.211(6)	Ru(1)–C(4)	2.281(6)
Ru(1)–C(5)	2.306(7)	2.316(7)	Ru(1)–C(6)	2.223(7)
Ru(1)–C(7)	2.225(7)	2.212(6)	Ru(1)–X(1)	2.5386(12)
C(5)–C(12)	1.455(10)	1.441(8)	C(12)–C(13)	1.522(9)
C(12)–C(20)	1.327(10)	1.348(8)	C(13)–X(2)	1.977(7)
			3	4
C(1)–Ru(1)–C(2)		89.6(3)		89.0(3)
C(1)–Ru(1)–X(1)		91.6(2)		88.0(2)
C(2)–Ru(1)–X(1)		90.4(3)		92.40(19)
C(12)–C(13)–X(2)		111.7(5)		112.8(4)
C(14)–C(13)–X(2)		109.3(5)		109.4(4)



Scheme 3.

The spectroscopic data of **3** and **4** are consistent with their structures. Both their IR spectra show two terminal carbonyl absorptions. In the downfield of the ^1H NMR spectra, two singlets at δ 7.13 and 5.88 ppm for **3** in CDCl_3 and at δ 6.57 and 5.74 ppm for **4** in $\text{C}_6\text{D}_5\text{CD}_3$ attributed to CH= and CHBr protons of the five-membered ring of indene are observed apart from the three multiplets for benzene ring. The corresponding signals in 1-bromoindene are at δ 6.82 and 5.48 ppm, respectively [22]. Three Cp protons are observed at δ 5.74–5.35 ppm for **3** and at δ 5.89–5.40 ppm for **4** together with a upfield singlet for the *tert*-butyl group.

(A) Cp and five-membered ring of indene



(B) ^tBu

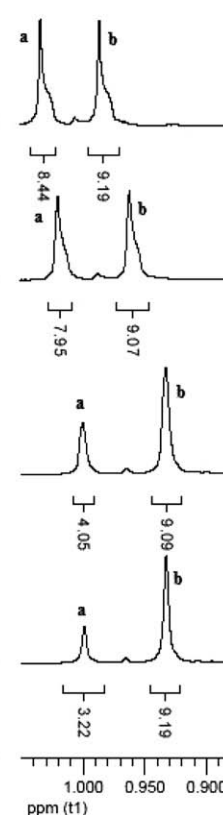


Fig. 4. Variable-temperature ^1H NMR spectra of $[\eta^5\text{-}(\text{tBuC}_5\text{H}_3)(\text{C}_9\text{H}_6\text{I})\text{Ru}(\text{CO})_2\text{I}]$ (**4**) in toluene- d_8 showing the signals for Cp and five-membered ring protons of indene (A) and for the ^tBu protons (B).

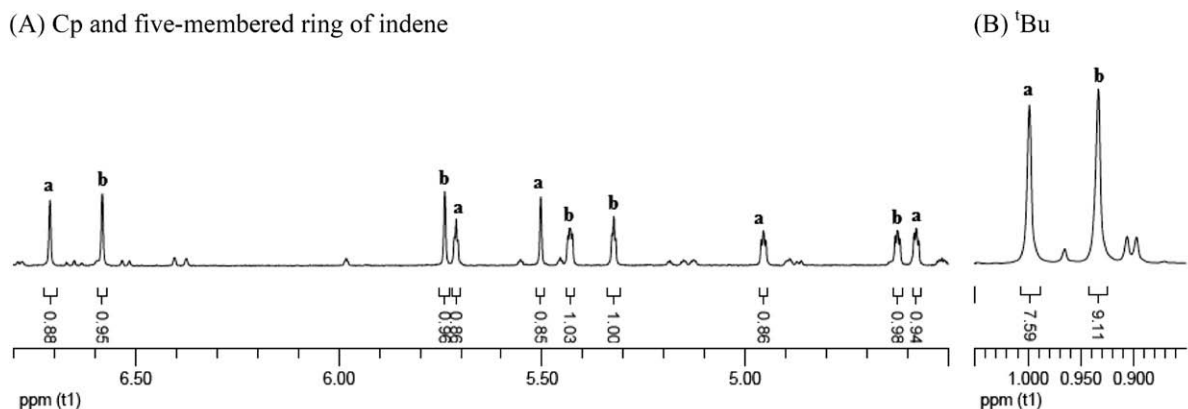
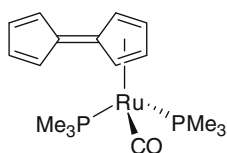


Fig. 5. ^1H NMR spectrum of $[\eta^5\text{-}(t\text{BuC}_5\text{H}_3)(\text{C}_9\text{H}_6\text{I})\text{Ru}(\text{CO})_2\text{I}]$ (**4**) in toluene- d_8 at 20 °C (the same sample of Fig. 4 was cooled down from 80 to 20 °C). The emergence of the little resonances might due to the decomposition.

It should note that their ^1H NMR spectra also show the existence of another species. It was shown that 1-substituted indenyls isomerize rapidly and quantitatively to 3-substituted indenyls in the basic condition via double-bond rearrangement [23]. But the chemical shifts of the other species (see Section 2) rule out such isomerization in our system. We presumed that they are probably the stereoisomers due to the orientation of the halogen atom bound to the indenyl group. As shown in Scheme 3, there are four isomers in theory for the mononuclear system $[(\eta^5\text{-}t\text{BuC}_5\text{H}_3)(\text{C}_9\text{H}_6\text{X})\text{Ru}(\text{CO})_2\text{X}]$. Among them **I** and **II**, **III** and **IV** are enantiomers, respectively. Therefore, two sorts of proton resonances were observed for the stereoisomers **a** and **b**. The two isomers could not be separated by column, or by recrystallization. The crystal structures of complexes **3** and **4**, as shown in Figs. 2 and 3, corresponding to isomer **II** and **I**, respectively. The variable-temperature ^1H NMR study of complex **4** showed that the ratio of isomers **a** and **b** increased from 0.4 to 0.9–1 as the temperature rising from 20 to 80 °C (Fig. 4). When the temperature fell down to 20 °C again, the ratio of isomers **a** and **b** was still ca. 0.9 and nearly no change (Fig. 5). This indicated that the two isomers could be interconverted with each other by the rotation about the C(5)–C(12) bond. However, due to that the indenyl ring and the Cp plane are almost coplanar and construct a conjugated unit, the rotation about the C(5)–C(12) bond should not be easy and need high temperature.

It is surprising that the reaction of **2** with halogen results in Ru cleavage from indenyl ring of the unsymmetrical Fv ligand. Vollhardt and co-workers have reported that reaction of $\text{FvRu}_2(\text{CO})_4$ with a large excess (8–10 equiv.) of PMe_3 afforded decomplexed system $\text{FvRu}(\text{PMe}_3)_3(\text{CO})$ (Scheme 4), in which only one Cp ring is bound to Ru [24]. Similar reaction was also proceeded in $\text{FvMo}_2(\text{CO})_6$ with strongly donating phosphines (PMe_3 , $\text{Me}_3\text{PCH}_2\text{PMe}_3$) [25,26]. But these reactions were still different from ours, since addition of a phosphine causes the simple substitution reaction while halogenation reaction is an oxidation process. The ligand induced metal cleavage from Cp ring was unambiguously established [6,7]. However, the similar cleavage of indenyl ring is rare [27]. At present we still cannot explain how the cleavage process takes place. Due to the ring slippage, the η^5 , η^3 , η^1 coordination modes



Scheme 4.

have been found for indenyl ligand and have been well characterized [28–36]. η^1 coordination mode is associated with fluxional behavior between the C1 and C3 bonding positions [35,36]. So the cleavage of Ru from the indenyl ligand of complex **2** might occur via $\eta^5 \rightarrow \eta^3 \rightarrow \eta^1$ ring slippage with the aid of excess halogen, although the intermediate complexes, such as η^3 or η^1 -coordinated species were not isolated.

In conclusion, reactions of $[\eta^5\text{-}\eta^5\text{-}(t\text{BuC}_5\text{H}_3)(\text{C}_9\text{H}_6)]\text{Ru}_2(\text{CO})_4$ (**2**) with excess halogens (Br_2 , I_2) afforded indenyl-decomplexed system $[(\eta^5\text{-}t\text{BuC}_5\text{H}_3)(\text{C}_9\text{H}_6\text{X})\text{Ru}(\text{CO})_2\text{X}]$ ($\text{X} = \text{Br}$, **3**; **I**, **4**). The reactions provide rare examples of halogen induced metal cleavage from indenyl ring.

Acknowledgments

This work was financially supported by NSFC (Grants 20702026, 20672058, and 20721062), Specialized Research Fund for the Doctoral Program of Higher Education (Grant 20070055020).

Appendix A. Supplementary material

CCDC 702932, 702933 and 702934 contain the supplementary crystallographic data for **2**, **3** and **4**. These data can be obtained free of charge from The Cambridge Crystallographic Data Centre via www.ccdc.cam.ac.uk/data_request/cif. Supplementary data associated with this article can be found, in the online version, at doi:10.1016/j.jorganchem.2008.12.058.

References

- [1] A. Ceccon, S. Santi, L. Orian, A. Bisello, *Coord. Chem. Rev.* 248 (2004) 683.
- [2] C.G. de Azevedo, K.P.C. Vollhardt, *Synlett* (2002) 1019.
- [3] M.-H. Delville, *Inorg. Chim. Acta* 291 (1999) 1.
- [4] P.A. McGovern, K.P.C. Vollhardt, *Synlett* (1990) 493.
- [5] D.L. Lichtenberger, N.E. Gruhn, M.E. Rempe, W.E. Geiger, T.T. Chin, *Inorg. Chim. Acta.* 240 (1995) 623.
- [6] J.M. O'Connor, C.P. Casey, *Chem. Rev.* 87 (1987) 307.
- [7] M.J. Calhorda, L.F. Veiros, *Coord. Chem. Rev.* 185–186 (1999) 37.
- [8] M.E. Rerek, L.N. Ji, F.J. Basolo, *Chem. Soc., Chem. Commun.* (1983) 1208.
- [9] R.C. Kerber, B.R. Waldbaum, *J. Organomet. Chem.* 513 (1996) 277.
- [10] R.C. Kerber, B. Waldbaum, *Organometallics* 149 (1995) 4742.
- [11] D. Tews, P.E. Gaede, *Organometallics* 20 (2001) 3869.
- [12] D. Tews, P.E. Gaede, *Organometallics* 23 (2004) 968.
- [13] P. Scott, U. Rief, J. Diebold, H.H. Brintzinger, *Organometallics* 12 (1993) 3094.
- [14] D. Tews, P.E. Gaede, *Tetrahedron Lett.* 45 (2004) 9029.
- [15] The chemical shift difference between the Cp-H protons of fulvalene ligands in ^1H NMR spectra appear to correlate with the presence of metal–metal bonding, as observed earlier: J.C. Smart, C.J. Curtis, *Inorg. Chem.* 16 (1977) 1788.

- [16] R. Boese, J.K. Cammack, A.J. Matzger, K. Pflug, W.B. Tolman, K.P.C. Vollhardt, T.W. Weidman, *J. Am. Chem. Soc.* 119 (1997) 6757.
- [17] K.P.C. Vollhardt, T.W. Weidman, *J. Am. Chem. Soc.* 105 (1983) 1676.
- [18] B. Li, B. Wang, S. Xu, X. Zhou, H. Song, *Organometallics* 25 (2006) 1158.
- [19] S.A.R. Knox, K.A. Macpherson, A.G. Orpen, M.C. Rendle, *J. Chem. Soc., Dalton Trans.* (1989) 1807.
- [20] S.A. Webott, A.K. Kakkar, G. Stringer, N.J. Taylor, T.B. Marder, *J. Organomet. Chem.* 394 (1990) 777.
- [21] M.A. Bennett, M.I. Bruce, T.W. Matheson, In G. Wilkinson, F.G.A. Stone, E.W. Abel (Eds.), *Comprehensive Organometallic Chemistry*, vol. 4, Pergamon Press, Oxford, New York, 1982, p. 281.
- [22] J.B. Woell, P. Boudjouk, *J. Org. Chem.* 45 (1980) 5213.
- [23] E.C. Freidrich, D.B. Taggart, *J. Org. Chem.* 40 (1975) 720.
- [24] R. Boese, W.B. Tolman, K.P.C. Vollhardt, *Organometallics* 5 (1986) 582.
- [25] M. Tilset, K.P.C. Vollhardt, *Organometallics* 4 (1985) 2230.
- [26] M. Tilset, K.P.C. Vollhardt, R. Boese, *Organometallics* 13 (1994) 3146.
- [27] A.A. Trifonov, E.A. Fedorova, I.A. Borovkov, G.K. Fukin, E.V. Baranov, J. Larionova, N.O. Druzhkov, *Organometallics* 26 (2007) 2488.
- [28] S.A. Westcott, A.K. Kakkar, G. Stringer, N.J. Taylor, T.B. Marder, *J. Organomet. Chem.* 394 (1990) 777.
- [29] J.S. Merola, R.T. Kacmarcik, D. Van Engen, *J. Am. Chem. Soc.* 108 (1986) 32.
- [30] T.C. Forschner, A.R. Cutler, R.K. Kullnig, *Organometallics* 6 (1987) 889.
- [31] R.M. Kowalewski, A.L. Rheingold, W.C. Trogler, F. Basolo, *J. Am. Chem. Soc.* 108 (1986) 2460.
- [32] L.F. Veiros, *Organometallics* 19 (2000) 3127.
- [33] O.J. Curnow, G.M. Fern, M.L. Hamilton, A. Zahl, R. van Eldik, *Organometallics* 23 (2004) 906.
- [34] C.C.L. Pereira, P.J. Costa, M.J. Calhorda, C. Freire, S.S. Rodrigues, E. Herdtweck, C.C. Romão, *Organometallics* 25 (2006) 5223. and references therein.
- [35] C.P. Casey, T.E. Vos, J.T. Brady, R.K. Hayashi, *Organometallics* 25 (2006) 5223.
- [36] W.A. Herrmann, F.E. Kühn, C.C. Romão, *J. Organomet. Chem.* 489 (1995) C56. and references therein.